MURDOCH RESEARCH REPOSITORY

http://researchrepository.murdoch.edu.au/21965/

Accepted Manuscript

The anodic dissolution of iron in ammoniacal-carbonate-thiosulfate-copper solutions with formation of Cu_2S and dendritic copper

Anna D'Aloya, Aleksandar N. Nikoloski

Please cite this article as: D'Aloya, Anna, Nikoloski, Aleksandar N., The anodic dissolution of iron in ammoniacal-carbonate-thiosulfate-copper solutions with formation of Cu_2S and dendritic copper, *Hydrometallurgy* (2014), doi: 10.1016/j.hydromet.2014.02.012
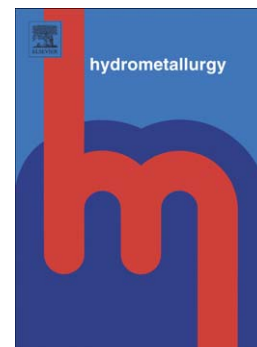
The anodic dissolution of iron in ammoniacal-carbonate-thiosulfate-copper solutions with formation of Cu_2S and dendritic copper

Anna D'Aloya and Aleksandar N. Nikoloski[*]

Murdoch University, South Street, Murdoch, WA 6150, Perth, Australia

Abstract

The presence of thiosulfate ions in ammoniacal-carbonate solutions containing copper(II) ions was found to prevent the passivation of iron, even though iron passivation is observed in solutions with no thiosulfate at very low copper(II) concentrations. The prolonged anodic dissolution of iron resulted in the formation of a partly crystalline sulfide layer on its surface, which based on Grazing Incidence X-Ray Diffraction (GI-XRD) analysis is thought to consist mainly of Cu_2S. The effect of the sulfide layer was investigated using rotating disk cyclic voltammetry. Unlike the formation of an amorphous CoS_x layer, which took place in similar solutions containing cobalt ions, the cuprous sulfide layer was not found to promote passivation of the iron. A significant amount of solid precipitate also became detached from the iron surface, remaining undissolved in the solution. This was analysed by X-Ray Diffraction (XRD) and scanning electron microscopy (SEM) – energy dispersive X-ray spectroscopy (EDX). Dendritic copper was observed both in the solid separated from the solution and in the precipitate still attached to the iron surface. The absence of iron passivation is thought to be due to both to the non-adherent nature of the cuprous sulfide layer, and to a disrupting effect caused by the cementation of copper.

Keywords: Ammonia; Leaching; Iron; Copper; Thiosulfate; Passivation; Nickel; Cobalt; Sulfide; Caron Process

1   Introduction

Ammoniacal solutions are often employed in hydrometallurgical processes due to their high selectivity towards the metal values. In the Caron process, nickeliferous laterites are roasted under reducing conditions in order to reduce the nickel and cobalt to the metallic state, and then leached in ammoniacal-carbonate solutions in order to dissolve the metal values as ammine complexes. During the reduction step, a significant amount of iron is also reduced to the metallic state, and forms alloys with the metal values. Therefore, the dissolution behaviour of these alloys, and hence the recovery of the metal values, is strongly influenced by the behaviour of iron. For this reason, numerous investigations have been conducted on the anodic behaviour of iron in ammoniacal solutions, with a particular focus on its active-passive behaviour both during polarisation experiments and under open circuit conditions (Jandova and Pedlik, 1991; Kho et al., 1992; Kim et al., 1991; Lee et al., 1985; Nicol et al., 2004; Nikoloski and Nicol, 2006; Nikoloski et al., 2003; Osseo-Asare et al., 1983).

Depending on the ore feed, the solutions involved in the Caron process contain variable amounts of dissolved metals, including at times copper, as well as metastable thiosulfate ions. These originate from the dissolution of sulfides formed during the reductive roast as a result of sulfur being present in the fuel. A previous study has shown that the dissolution of iron is significantly suppressed, with a tendency to passivate, in solutions containing both dissolved cobalt and thiosulfate ions (Nikoloski et al., 2003; D'Aloya and Nikoloski, 2013). This behaviour was attributed to the progressive coverage of the iron surface by a cobalt sulfide or polysulfide layer, which appears to play a key role in the passivation mechanism. The study was particularly relevant to the QNi Caron plant in Yabulu, Australia, where cobalt and thiosulfate ions appear to be the main species influencing the anodic behaviour of iron. It is also relevant because cobalt losses into such layers may further affect the process efficiency. On the other hand, the typical dissolved copper concentrations found in the leach liquor at the Yabulu plant are quite low.

More significant amounts of copper may be encountered in ammoniacal-carbonate solutions employed in the processing of ores richer in copper, such as at the Votorantim Metais plant in Brazil. A previous study has found that iron readily passivates in the presence of millimolar amounts of dissolved copper (D'Aloya and Nikoloski, 2012). However studies conducted in ammoniacal-carbonate solutions containing both copper (II) and thiosulfate ions are complicated by the possibility of a homogeneous redox reaction between these two species (Rábai and Epstein,

[*] Corresponding author. Tel.: + 61 8 9360 2835; fax: + 61 8 9360 6343.

E-mail address: A.Nikoloski@murdoch.edu.au (A. N. Nikoloski).

1992). The oxidation of thiosulfate by copper (II) in the presence of ammonia has been studied extensively due to its relevance to the ammoniacal leaching of metal sulfides and to the thiosulfate leaching of gold, which is enhanced by the addition of copper (II) and ammonia (Breuer and Jeffrey, 2003; Byerley et al., 1973a,b, 1975). The reaction is known to produce tetrathionate, which then undergoes further oxidative degradation resulting mainly in sulfate and trithionate, and cuprous thiosulfate, ammine or mixed complexes, depending on the relative concentrations of ammonia and thiosulfate. In the presence of oxygen, the copper (I) species are re-oxidised to copper (II) ammines, which therefore function as redox mediators, resulting in much higher rates of thiosulfate degradation. The reaction rate is known to be significantly lower at higher ammonia concentrations, such as those employed in the Caron process.

The present study focusses on the interaction between metallic iron and both copper and thiosulfate ions under conditions similar to those encountered in the Caron process. Based on the results obtained, it was possible to identify some of the main reactions involved.

2   Experimental details

The electrochemical measurements were recorded using a three electrode jacketed cell connected to a 6310 EG&G Princeton Applied Research potentiostat. The working electrode was a rotating disk electrode (RDE) made of 99.98% polycrystalline iron, rotating at a speed of 500 rpm. The counter electrode was a platinum wire and the reference electrode was a saturated calomel electrode (SCE). This was placed in a Luggin capillary filled with the cell solution and placed with its tip a few millimetres away from the working electrode, in order to minimise the effect of solution resistance. All of the potentials reported in this study were converted to the standard hydrogen electrode (SHE) scale. The jacketed cell was connected to a thermostat-controlled water bath set to 45°C in order to simulate the Caron process temperature. All of the solutions used in this study were prepared using deionised water and AR grade aqueous ammonia, ammonium bicarbonate, copper sulfate and sodium thiosulfate. Concentrations reported in the text as $[NH_3]_T$ and $[CO_2]_T$ refer to the total concentration of ammonia and carbonate species respectively, which resulted in a solution pH of around 10.5. The copper and thiosulfate species concentrations are referred to as $[Cu(II)]$ and $[S_2O_3^{2-}]$ for simplicity, although they are expected to undergo various redox transformations once in solution. Since the presence of dissolved oxygen was not found to have a significant effect on the observed behaviour, the solutions employed for the experiments reported were not sparged with nitrogen, in order to maintain a more accurate control of the ammonia concentration.

The grazing incidence X-ray diffraction (GIXRD) pattern was recorded using a Panalytical Empyrean diffractometer, while the normal incidence XRD was obtained using a GBC EMMA diffractometer. The microscope images and elemental analyses were obtained using a Philips XL20 scanning electron microscope (SEM) combined with an Oxford Link ISIS 5175 energy dispersive X-ray spectroscopy (EDX) detector. The UV-Visible spectra were obtained using a HP 8453 spectrophotometer with 1 and 0.1 cm path length quartz cells for the lower and higher [Cu(II)] respectively. The experiments carried out in order to obtain samples for the XRD and UV-Visible characterisation studies were conducted at room temperature in a closed glass vessel, in which the solution was stirred by a magnetic stirrer. A 99% iron disk was attached to the lid of the vessel, in such manner that no air was present above the solution during the experiment. All of the iron surfaces were polished immediately prior to immersion using 1200 grit silicon carbide paper wetted with ammonia-ammonium bicarbonate solution.

3   Results

3.1   OCP Measurements

The OCP of an iron rotating disk electrode was found to remain in the active dissolution region of iron in ammoniacal–carbonate solutions, throughout a number of 3 hour measurements conducted using various copper (II) concentrations between 1 mM and 12 mM, and thiosulfate concentrations between 4 mM and 24 mM. This behaviour can be seen for example in Figure 1 (curve a). By comparison, the OCP behaviour with the same copper (II) concentration but with no thiosulfate (curve (b)) shows a distinct transition due to the passivation of iron.

Figure 1. OCP of Fe in 5 M $[NH_3]_T$, 1 M $[CO_2]_T$ and a) 12 mM [Cu (II)], 22 mM $[S_2O_3^{2-}]$; b) 12 mM [Cu (II)].

During dissolution, the formation of a black solid on the iron surface was also observed. This was found to be non-adherent and to continuously fall off the iron surface, remaining suspended in the agitated solution. Sharp drops in the OCP of up to 50 mV were observed each time a piece of the black solid layer became detached from the iron surface. The precipitation of significant amounts of finely divided iron (III) hydroxides was also observed.

In solutions containing cobalt and thiosulfate ions, the presence of copper ions, even at very low concentrations, was found to significantly delay the onset of passivation. For example, a copper concentration as low as 0.1 mM in an ammoniacal-carbonate solution containing 12 mM [Co(II)] and 24 mM $[S_2O_3^{2-}]$ resulted in the passivation taking place after 2 hours of immersion, as opposed to the 30-40 minutes it took when no copper ions were added (Figure 2).

Figure 2. OCP of Fe in 3 M $[NH_3]_T$, 1 M $[CO_2]_T$, 12 mM [Co(II)], 24 mM $[S_2O_3^{2-}]$ and a) no Cu(II); b) 0.1 mM [Cu(II)].

In a final experiment, an iron RDE which had been allowed to passivate in an ammoniacal-carbonate solution containing copper(II) but no thiosulfate was then immersed in ammoniacal-carbonate solutions containing both copper(II) and thiosulfate ions. In this case, the OCP measurements on the iron RDE showed that it remained passive.

3.2   XRD and SEM/EDX Analysis

As the OCP behaviour did not exhibit significant differences across the concentration ranges of copper and thiosulfate, XRD and SEM/EDX analysis was only carried out for one representative combination. The iron RDE immersed for 3 hours in an ammoniacal-carbonate solution containing 12 mM Cu(II) and 24 mM thiosulfate ions was analysed. SEM-EDX analysis of its surface revealed the presence of a predominantly dendritic deposit, with an elemental analysis of approximately 30% Cu and 20% S. An iron RDE immersed for 4 hours under the same conditions was analysed by GIXRD, which revealed the presence of metallic copper and Cu_2S (Figure 3).

Figure 3. GIXRD (Cu Kα) pattern of the Fe RDE following immersion in 5 M $[NH_3]_T$, 1 M $[CO_2]_T$, 12 mM [Cu(II)] and 24 mM $[S_2O_3^{2-}]$.

The solid precipitate which formed following immersion of the iron RDE in the absence of air above the solution was also analysed. SEM images of the filtered solid revealed a mixture of phases with different morphologies (Figure 4) and the EDX elemental analysis resulted in major variations in the relative amounts of copper and sulfur in different parts of the precipitate. XRD analysis of the solid indicated the presence of metallic copper, Cu_2O, Cu_2S, possibly $CuFe_4S_7$ and FeS (Figure 5).

Figure 4. SEM images of the solid precipitate formed during the dissolution of iron in 6 M $[NH_3]_T$, 2 M $[CO_2]_T$, 12 mM [Cu(II)] and 24 mM $[S_2O_3^{2-}]$.

Figure 5. XRD (Cu Kα) pattern of the solid precipitate formed during the dissolution of iron in 6 M $[NH_3]_T$, 2 M $[CO_2]_T$, 12 mM [Cu(II)] and 24 mM $[S_2O_3^{2-}]$.

3.3 UV-VIS Spectrophotometric Analysis

In order to provide reference data to enable a determination of whether the reduction of copper (II) by thiosulfate ions occurred to a significant extent at the ammonia concentrations used for this study, reference solutions containing ammonia, carbonate, copper (II) and/or thiosulfate ions were investigated using UV-VIS spectrophotometry. The results are to be treated qualitatively, due to reaction between the species during solution preparation and due to the presence of dissolved oxygen, which re-generated copper (II) tetrammine following its reduction.

Spectra were first obtained for copper (II) in 6 M $[NH_3]_T$, 2 M $[CO_2]_T$ solution. This resulted in a maximum UV absorption at 246 nm and a broad absorption in the visible region at 630 nm, which is due to the formation of a blue cupric ammine complex (Figure 6, solid line). Spectra were then obtained for copper (II) in 24 mM aqueous sodium thiosulfate. This resulted in a UV absorption maximum at 276 nm, thought to be due to a cuprous thiosulfate complex (Figure 6, dotted line), possibly formed from the reduction of copper by thiosulfate as follows:
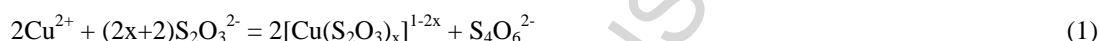
$$2Cu^{2+} + (2x+2)S_2O_3^{2-} = 2[Cu(S_2O_3)_x]^{1-2x} + S_4O_6^{2-} \tag{1}$$

Figure 6. UV-VIS spectra of 4 mM Cu (II) in 6 M $[NH_3]_T$, 2 M $[CO_2]_T$ (solid line), and in 24 mM $[S_2O_3^{2-}]$(dotted line).

A study was then conducted for copper (II) in 24 mM $[S_2O_3^{2-}]$, 3 M $[NH_3]_T$ and 1 M $[CO_2]_T$, which corresponds to half the $[NH_3]_T$ and $[CO_2]_T$ employed in the study with an iron RDE. The spectra indicated the presence of both a copper (II) ammine complex, with a maximum absorbance at 623 nm, and a Cu(I) thiosulfate complex, with a peak at 273 nm (Figure 7, solid line). The intensity of these two peaks was monitored over a 2.5 hour period (Figure 7, dotted lines), during which the absorbance peak at 273 nm was found to decrease by over 17%, suggesting the progressive consumption of thiosulfate ions by reaction with copper (II). A decrease of just over 6% in the cupric tetrammine absorbance at 623 nm was also observed, despite its rapid regeneration by reaction with oxygen.

Figure 7. UV-visible spectrum of 4 mM Cu (II) in 24 mM $[S_2O_3^{2-}]$, 3 M $[NH_3]_T$ and 1 M $[CO_2]_T$ (solid line); change over time in maximum absorbance at 273 nm and 623 nm (dotted lines).

At 6 M $[NH_3]_T$, 2 M $[CO_2]_T$, the UV-visible measurements were conducted at the highest $[S_2O_3^{2-}]$ and [Cu(II)] used in the studies with an iron RDE, and in a tightly sealed cell with no air above the solution. This minimised the loss of ammonia and re-oxidation of Cu(I). The higher Cu(II) concentration made it necessary to use a shorter path-length of 0.1 cm. The spectrum was found to be qualitatively similar to that of copper (II) in ammoniacal carbonate solutions (Figure 8, solid line), with no absorbance peak arising from the presence of thiosulfate ions. Despite the presence of dissolved oxygen, it was possible to observe a clear decrease over time in cupric tetrammine absorbance at 620 nm (Figure 8, dotted line), suggesting that the homogeneous reduction of cupric ammines by thiosulfate took place to an appreciable extent even at the high $[NH_3]_T$ employed in this study.

Figure 8. UV-VIS spectrum of 12 mM Cu (II) in 24 mM $[S_2O_3^{2-}]$, 6 M $[NH_3]_T$ and 2 M $[CO_2]_T$ (solid line); change over time in maximum absorbance at 620 nm (dotted line).

UV-VIS Spectrophotometric analysis of the solution was also carried out following the immersion of metallic iron at room temperature, with no air above the solution. Within approximately half an hour of immersion and active dissolution of the iron, the solution colour changed from deep blue to colourless, indicating the rapid reduction of most of the copper (II) ammine complexes to copper (I) species and metallic copper.

The UV-visible spectrum, measured using a 0.1 cm path length, is shown in Figure 9. As expected, there was no visible absorbance in the 620 nm region, indicating complete reduction of the cupric ammines. This appeared to be sustained by the iron remaining in its active dissolution state throughout the experiment, rather than by reaction with thiosulfate ions. Under such conditions, dissolved oxygen was also consumed by metallic iron, so the concentration of cupric tetrammine continued to decrease as its regeneration was not sustained by reaction with dissolved oxygen.

This is supported by the colour change which was only observed when the iron disk was activated by polishing immediately prior to immersion, a condition which replicated the initial stages of the Caron leach.

The maximum UV absorbance at 269 nm was attributed to a cuprous thiosulfate complex, which was not observed following the homogeneous reaction in the absence of iron. This confirmed that there was practically no dissolved oxygen available to reoxidise the complex, and that the cupric ammines were reduced predominantly by iron rather than thiosulfate.

Therefore, the homogeneous reduction of copper (II) by thiosulfate is not expected to significantly affect the studies conducted in the presence of metallic iron, nor to take place to a significant extent during the initial stage of the Caron leach.

Figure 9. UV-VIS spectrum of 12 mM Cu (II), 24 mM $[S_2O_3^{2-}]$, 6 M $[NH_3]_T$ and 2 M $[CO_2]_T$ solution following reaction with metallic iron.

3.4   Rotating disk cyclic voltammetry

The voltammetric response of the iron RDE was measured following 15 minutes of immersion in 6 M $[NH_3]_T$, 2 M $[CO_2]_T$ solutions at different [Cu(II)] and $[S_2O_3^{2-}]$ (Figure 10). For the purpose of this investigation, it was not necessary to compensate the results for the solution resistance between the tip of the Luggin capillary and the RDE surface. Therefore, at high anodic currents there appears to be slight shifts with respect to the potential, resulting from changes in the solution conductivity at different species concentrations.

Scanning the potential in the positive direction from the OCP resulted in an anodic peak due to the dissolution of metallic iron (A) in the -0.6 V to -0.2 V potential region, followed by a smaller anodic process (B) in the -0.1 V to 0 V region and a third peak (C) above 0.1 V. The peak current density at A was not significantly affected by changes in the [Cu(II)] and $[S_2O_3^{2-}]$, whereas increasing [Cu(II)] from 1 mM to 4 mM at constant $[S_2O_3^{2-}]$ resulted in a 7-fold increase in peak C. Further increase to 12 mM had a smaller effect on the peak current density, but resulted in a fourth anodic process (D) being observed in the 0.4 V to 0.5 V potential region, as a shoulder following peak C. On the other hand, increasing $[S_2O_3^{2-}]$ at constant [Cu(II)] resulted in a 10% decrease in the current density at peak C. These observations are consistent with peak C being due to the oxidation of a copper-containing species, such as a copper sulfide, formed during the anodic dissolution of iron. Its formation appears to be strongly dependent on the copper (II) concentration, as consistent with the change in peak current density, whereas the effect of $[S_2O_3^{2-}]$ may be explained in terms of a decrease in [Cu(II)] by reaction with thiosulfate ions. This suggests that the species responsible for peak C may possibly form as a result of copper (II) reduction to copper (I) on the iron surface. Following reversal of the potential scan, the RDE appeared to become passive, with no significant current being observed in the cathodic direction until it reached negative values. Scanning the potential below 0V resulted in a cathodic process, likely to be the reduction of cupric ammines, followed by a further increase in cathodic current density observed at higher [Cu(II)] as the potential approached -0.4 V. The anodic dissolution of metallic iron resumed in the region of -0.4 V (A[1]), reaching higher current densities at lower [Cu(II)] and higher $[S_2O_3^{2-}]$.

Figure 10. Rotating disk cyclic voltammetry (50 mV/s) of the Fe RDE following 15 minutes of immersion in 6 M $[NH_3]_T$, 2 M $[CO_2]_T$ and a) 1 mM [Cu(II)] and 4 mM $[S_2O_3^{2-}]$; b) 4 mM [Cu(II)] and 4 mM $[S_2O_3^{2-}]$; c) 12 mM [Cu(II)] and 4 mM $[S_2O_3^{2-}]$ (solid line); 4 mM [Cu(II)] and 24 mM $[S_2O_3^{2-}]$ (dotted line).

Cyclic voltammetric measurements taken after 2 hours of immersion resulted in a continued increase in anodic current density in the potential region of (C), which did not result in a peak prior to reaching the inversion potential, as shown in Figure 11 for 4 mM [Cu(II)] and 24 mM $[S_2O_3^{2-}]$. The cathodic scan, resulted in a similar but lower anodic current due to the process at C, and a negative current as the potential was decreased below 0.1. Two cathodic peaks were observed, one between 0 and -0.1 V (E) and the other just below -0.4 V (F), while the reactivation of metallic iron (A[1]) was not observed in this case.
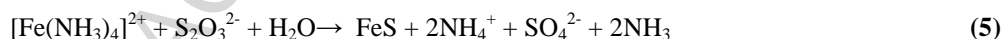
Figure 11. Rotating disk cyclic voltammetry (50 mV/s) of the Fe RDE in 6 M $[NH_3]_T$, 2 M $[CO_2]_T$, 4 mM [Cu(II)] and 24 mM $[S_2O_3^{2-}]$ taken after 2 hours of immersion.

Monitoring the voltammetric response following different periods of immersion at 4 mM [Cu(II)] and 4 mM [$S_2O_3^{2-}$] showed a progressive increase in current density at C (Figure 12). For the 2 hour immersion, inversion of the scan at the same potential as the other measurements resulted in a similar response as that shown in Figure 11, although in this case the reactivation of metallic iron (A^1) was observed. By inverting the scan at a higher potential, it was possible to observe a very large peak C, as can be seen in Figure 12. These results indicate that although a substantial amount of the species being oxidised at C is formed during the anodic dissolution of iron, this does not appear to promote the passivation of iron, nor to significantly suppress its dissolution.

Figure 12. Rotating disk cyclic voltammetry (50 mV/s) of the Fe RDE in 6 M [NH$_3$]$_T$, 2 M [CO$_2$]$_T$, 4 mM [Cu(II)] and 4 mM [S$_2$O$_3$$^{2-}$] taken immediately after immersion (I), after 10 minutes of immersion (II) and after 2 hours of immersion (III).
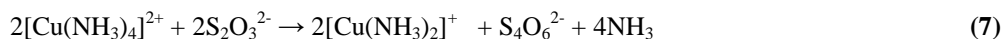
4   Discussion of reactions

In the absence of thiosulfate ions, the dissolution of iron in ammoniacal-carbonate solutions containing copper (II) ions can be described by reactions (2-4). When thiosulfate ions are present, the presence of metallic copper on the iron surface as observed by GIXRD indicates that these reactions still take place. The thiosulfate ions are also thought to act as oxidants in the dissolution of iron, and have been found to significantly enhance it, as suggested by the resulting higher anodic current densities reported by D'Aloya and Nikoloski, 2013.

$$Fe + 2[Cu(NH_3)_4]^{2+} \rightarrow [Fe(NH_3)_4]^{2+} + 2[Cu(NH_3)_2]^+ \qquad (2)$$

$$Fe + [Cu(NH_3)_4]^{2+} \rightarrow [Fe(NH_3)_4]^{2+} + Cu \qquad (3)$$

$$Fe + 2[Cu(NH_3)_2]^+ \rightarrow [Fe(NH_3)_4]^{2+} + 2Cu \qquad (4)$$

The detection of a small amount of sulfur by SEM/EDX analysis of the iron surface following immersion in the presence of thiosulfate, and the production of H$_2$S upon addition of HCl, indicates that some sulfide was adsorbed on the iron surface, with the formation of an iron sulfide or polysulfide. It has been suggested that during the initial stage of the Caron leach, iron sulfide may form via the disproportionation of thiosulfate (Queneau and Weir, 1986) which may be described by reaction 5. Similarly, it was suggested that the precipitation of even less soluble metal sulfides took place via an analogous mechanism involving other metal ions present in the leach solution. However, the formation of metal sulfides was only observed on the electrode surface, suggesting that it is more likely to involve the reduction of thiosulfate by metallic iron. In such case, the formation of iron sulfide may be described by reaction 6.

$$[Fe(NH_3)_4]^{2+} + S_2O_3^{2-} + H_2O \rightarrow FeS + 2NH_4^+ + SO_4^{2-} + 2NH_3 \qquad (5)$$

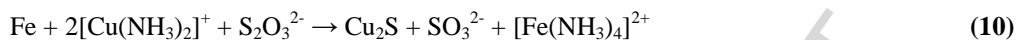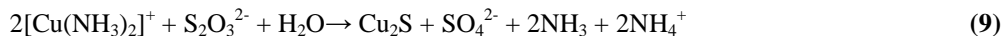$$Fe + S_2O_3^{2-} \rightarrow FeS + SO_3^{2-} \qquad (6)$$

When both thiosulfate and copper (II) ions are present, the picture is potentially more complicated, due to the well known homogeneous redox reaction between copper (II) and thiosulfate ions, which may result in the formation of various cuprous thiosulfate, ammine and mixed complexes, depending on the relative ammonia and thiosulfate concentrations. This may be described by reactions 7 and 8, where thiosulfate is initially oxidised to tetrathionate, which is then further oxidised resulting in a mixture of sulfur oxyanions.

$$2[Cu(NH_3)_4]^{2+} + 2S_2O_3^{2-} \rightarrow 2[Cu(NH_3)_2]^+ + S_4O_6^{2-} + 4NH_3 \qquad (7)$$

$$2[Cu(NH_3)_4]^{2+} + 4S_2O_3^{2-} \rightarrow 2[Cu(S_2O_3)]^- + S_4O_6^{2-} + 8NH_3 \qquad (8)$$

However, in the presence of metallic iron, the copper (I) complexes are thought to result mainly from reaction 1, as discussed in section 3.3. The formation of Cu$_2$S may then take place by further reaction of cuprous complexes and disproportionation of thiosulfate (reaction 9). However, since its formation was only observed in the presence of metallic iron, the overall process is better described by reaction 10. It is also possible that some Cu$_2$S was formed by the reduction of thiosulfate on the copper dendrites formed by reactions 3 and 4, as described by reaction 11. Similar

mechanisms may be responsible for the formation of mixed iron-copper sulfides and of various other unidentified or amorphous sulfide or polysulfide species.

$$2[Cu(NH_3)_2]^+ + S_2O_3^{2-} + H_2O \rightarrow Cu_2S + SO_4^{2-} + 2NH_3 + 2NH_4^+ \tag{9}$$

$$Fe + 2[Cu(NH_3)_2]^+ + S_2O_3^{2-} \rightarrow Cu_2S + SO_3^{2-} + [Fe(NH_3)_4]^{2+} \tag{10}$$

$$2Cu + S_2O_3^{2-} \rightarrow Cu_2S + SO_3^{2-} \tag{11}$$

5   Conclusions

When both copper (II) and thiosulfate ions are present in ammoniacal-carbonate solutions, the passivation of iron is suppressed, unlike the behaviour observed in analogous solutions containing either copper (II) ions or both cobalt (II) and thiosulfate ions. The OCP of an iron rotating disk electrode was found to remain in the active dissolution region of iron in ammoniacal–carbonate solutions, throughout a number of 3 hour measurements at variable copper (II) and thiosulfate concentrations.

During dissolution, a non-adherent black solid layer was formed on the iron surface, and found to contain Cu_2S and dendritic copper. The effect of this layer was studied using rotating disk cyclic voltammetry and a significant amount of it was found to remain in electrical contact with the iron RDE surface. It is remarkable that in this case, the formation of such a sulfide deposit on the iron surface did not appear to suppress the dissolution of iron, as it had in the case of CoS_x, nor was it found to promote its passivation. This is thought to be due to the partly crystalline, non-adherent nature of the deposit, and possibly to a disrupting effect of the cementation of copper.

Acknowledgements

References

Breuer, P.L. and Jeffrey, M.I., 2003. The reduction of copper(II) and the oxidation of thiosulfate and oxysulfur anions in gold leaching solutions. Hydrometallurgy 70, 163-173.

Byerley, J.J., Fouda, S.A. and Rempel, G.L., 1973a. Kinetics and mechanism of the oxidation of thiosulfate ions by copper (II) ions in aqueous ammonia solution. Journal of the Chemical Society, Dalton Transactions, 889-893.

Byerley, J.J., Fouda, S.A. and Rempel, G.L., 1973b. The oxidation of thiosulfate in aqueous ammonia by copper (II) oxygen complexes. Inorganic and Nuclear Chemistry Letters 9, 879-883.

Byerley, J.J., Fouda, S.A. and Rempel, G.L., 1975. Activation of copper (II) ammine complexes by molecular oxygen for the oxidation of thiosulfate ions. Journal of the Chemical Society, Dalton Transactions, 1329-1338.

D'Aloya, A. and Nikoloski, A.N., 2013. An electrochemical investigation of the formation of CoS_x and its effect on the anodic dissolution of iron in ammoniacal-carbonate solutions. Hydrometallurgy 131-132, 99-106.

D'Aloya, A. and Nikoloski, A.N., 2012. The passivation of iron in ammoniacal solutions containing copper (II) ions. Hydrometallurgy 111-112, 58-64.

Jandova, J. and Pedlik, M., 1991. Anodic dissolution of iron-nickel, iron-cobalt, and nickel-cobalt alloys in ammoniacal ammonium carbonate solutions. Hutnicke Listy 46, 75-81.

Kho, Y.T., Osseo-Asare, K. and Pickering, H.W., 1992. Anodic behavior of iron in ammoniacal carbonate solution. I. Steady-state polarization and cyclic voltammetry. Journal of the Electrochemical Society 139, 32-39.

Kim, H.S., Kho, Y.T., Osseo-Asare, K. and Pickering, H.W., 1991. Active and passive behavior of sintered iron in ammoniacal ammonium carbonate solution. Metallurgical Transactions B, 22B, 323-332.

Lee, J.W., Osseo-Asare, K. and Pickering, H.W., 1985. Anodic dissolution of iron in ammoniacal ammonium carbonate solution. Journal of the Electrochemical Society 132, 550-5.

Nicol, M.J., Nikoloski, A.N. and Fittock, J.E., 2004. A fundamental study of the leaching reactions involved in the Caron process. In: Imrie, W.P., Lane, D.M. (Eds), International Laterite Nickel Symposium, TMS, Warrendale, Pennsylvania, pp. 369-384.

Nikoloski, A.N. and Nicol, M.J., 2006. The electrochemistry of the leaching reactions in the Caron process. I. anodic processes. In: Doyle, F.M., Kelsall, G.H., Woods, R. (Eds.), Electrochemistry in Mineral and Metal Processing VII, ECS, Pennington, New Jersey, pp. 197-207.

Nikoloski, A.N., Nicol, M.J. and Fittock, J.E., 2003. The passivation of iron during the leaching of pre-reduced laterite ores in ammoniacal solutions. In: Doyle, F.M., Kelsall, G.H., Woods, R. (Eds.), Electrochemistry in Mineral and Metal Processing VI, ECS, Pennington, New Jersey, pp. 205-218.

Osseo-Asare, K., Lee, J.W., Kim, H.S. and Pickering, H.W., 1983. Cobalt extraction in ammoniacal solution: electrochemical effect of metallic iron. Metallurgical Transactions B, 14B, 571-576.

Queneau, P.B. and Weir, D.R., 1986. Control of iron during hydrometallurgical processing of nickeliferous laterite ores. In: Dutrizac, J.E., Mohemius, A.J. (Eds.), Iron Control in Hydrometallurgy, Ellis Horwood Ltd., Chichester, U.K., pp. 76-105.

Rábai, G. and Epstein, I.R., 1992. Equilibria and kinetics of the fast interaction between copper (II) and thiosulfate ions in aqueous solution. Inorganic Chemistry 31, 3239-3242.
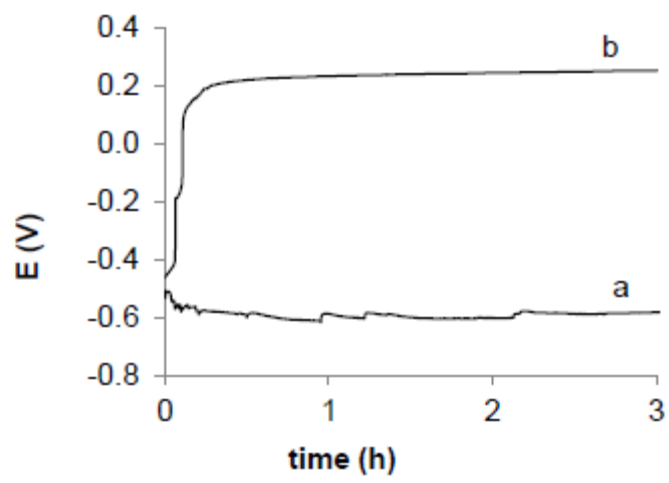
Figure 1

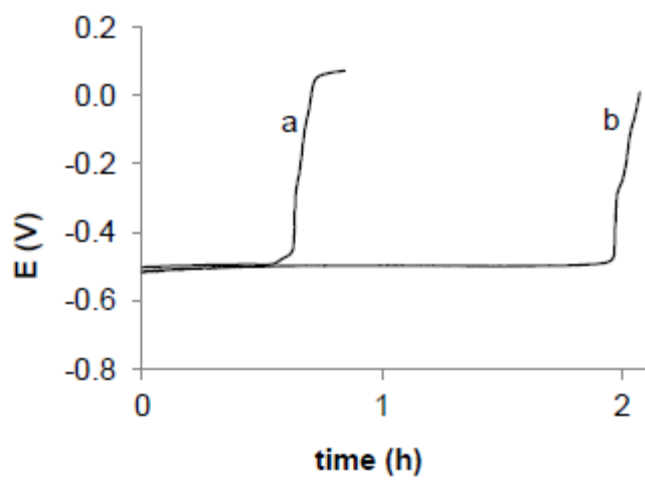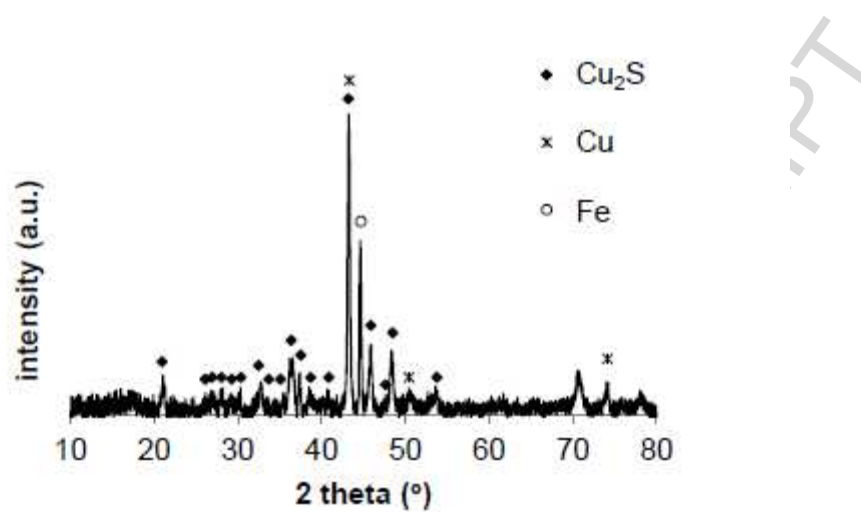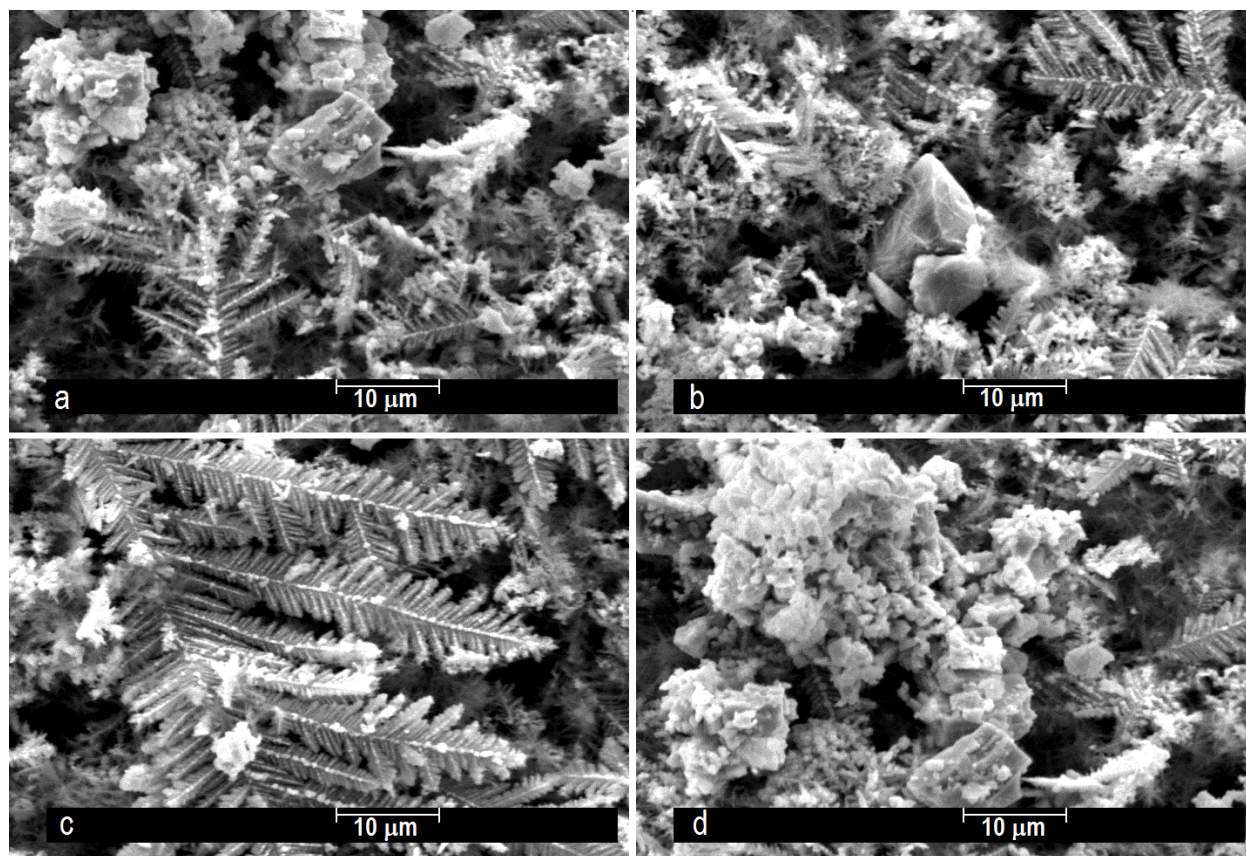**Figure 2**

Figure 3

Figure 4
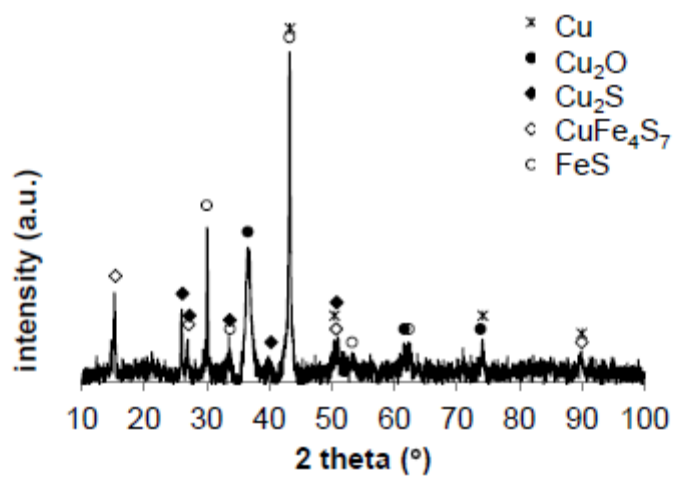
Figure 5
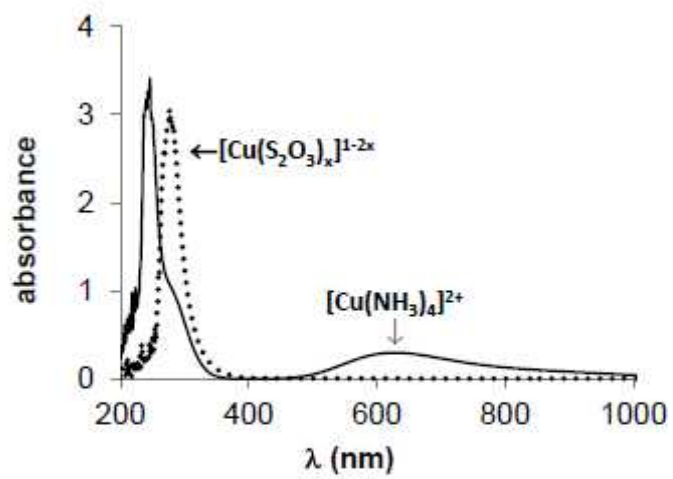
Figure 6
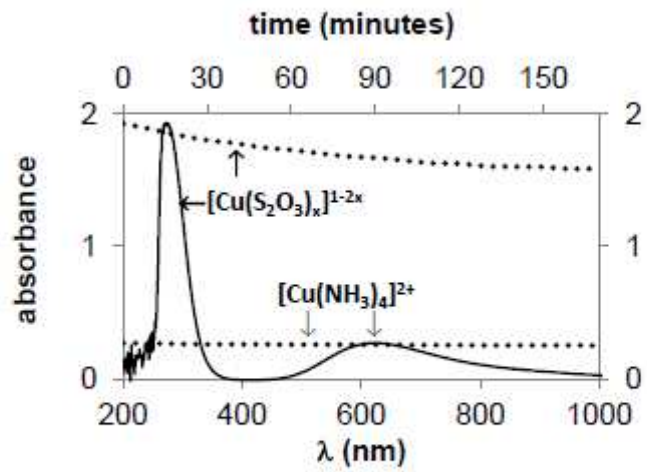
Figure 7
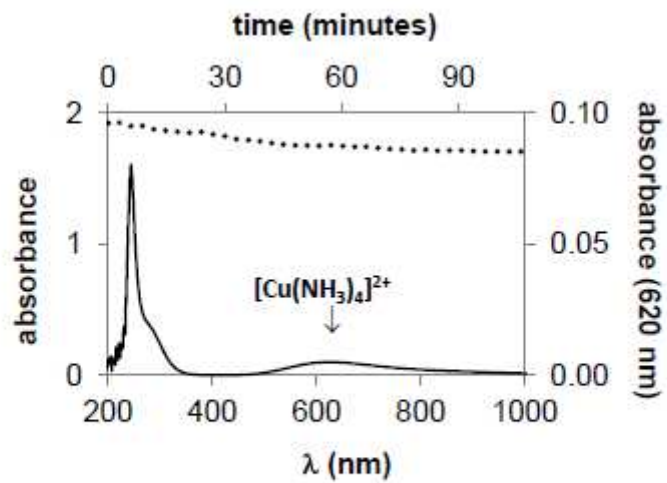
Figure 8
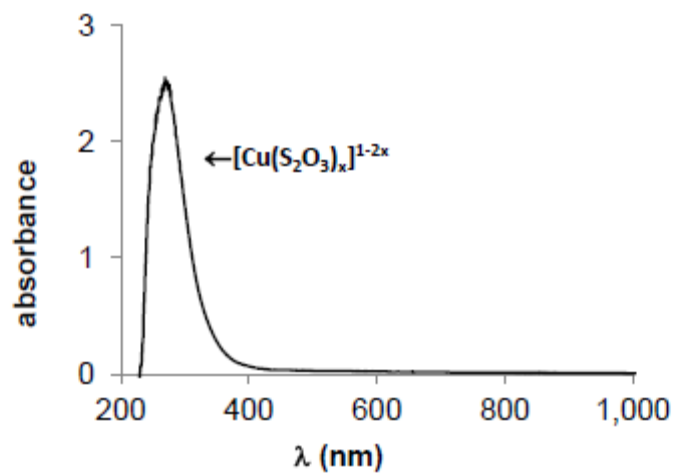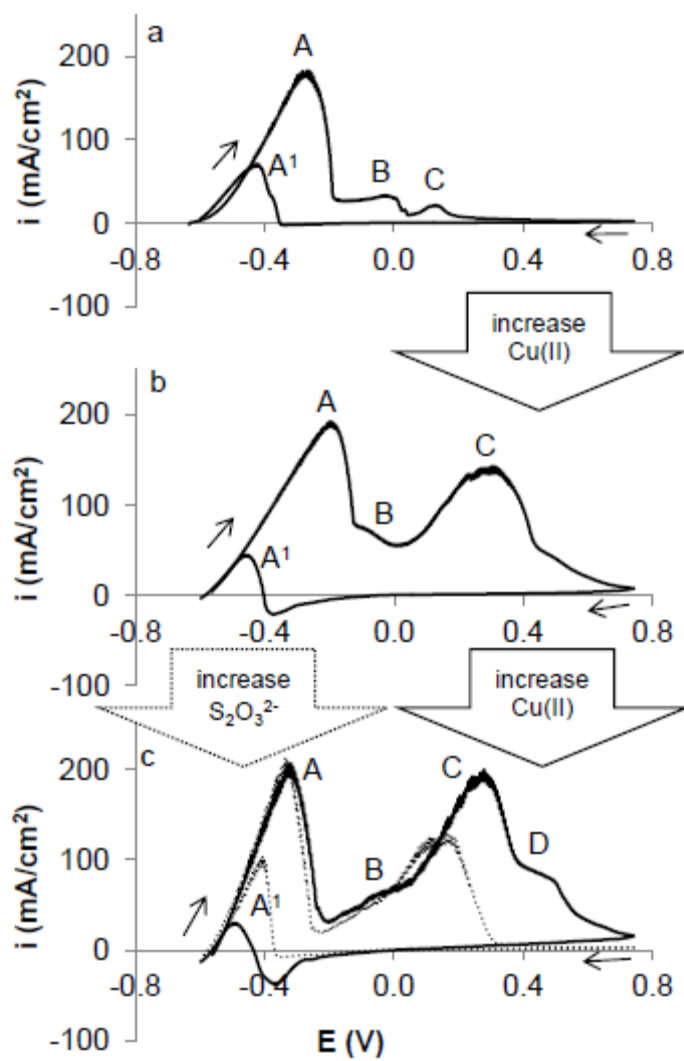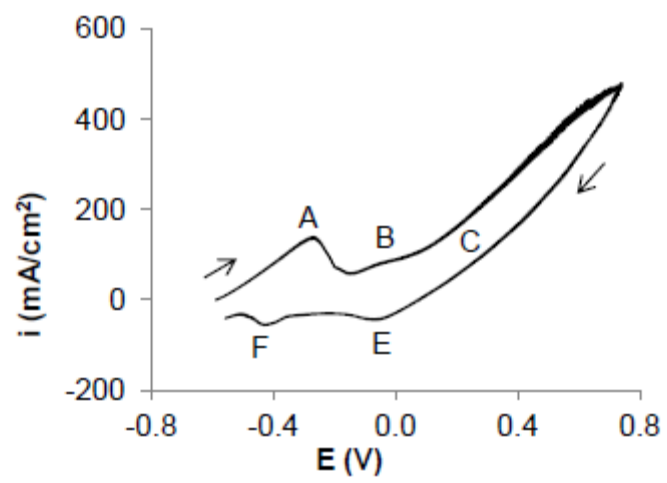
Figure 9

Figure 10

Figure 11

Figure 12

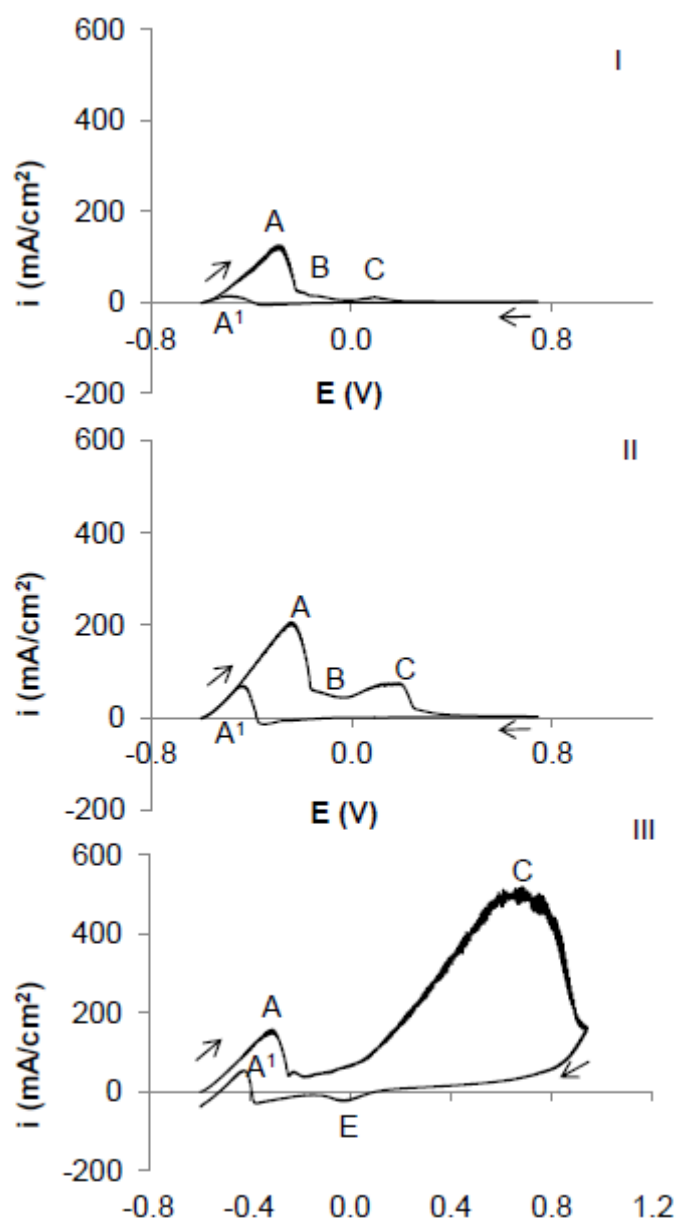**Highlights**

- $S_2O_3^{2-}$ prevents the passivation of Fe by Cu(II) in aqueous NH_3/NH_4HCO_3
- Non-adherent surface layer containing Cu dendrites and Cu_2S forms on Fe surface
- Solid layer remains undissolved in solution following detachment